Density dependence of the room temperature thermal conductivity of atomic layer deposition-grown amorphous alumina (Al2O3)

Caroline S. Gorham, John T. Gaskins, Gregory N. Parsons, Mark D. Losego, and Patrick E. Hopkins

Articles you may be interested in

Growth of crystalline Al2O3 via thermal atomic layer deposition: Nanomaterial phase stabilization
APL Mat. 2, 032105 (2014); 10.1063/1.4868300

Deposition temperature dependence of material and Si surface passivation properties of O3-based atomic layer deposited Al2O3-based films and stacks
J. Vac. Sci. Technol. A 32, 01A128 (2014); 10.1116/1.4852855

Atomic rearrangements in amorphous Al2O3 under electron-beam irradiation
J. Appl. Phys. 113, 064312 (2013); 10.1063/1.4790705

Modulation of atomic-layer-deposited Al2O3 film passivation of silicon surface by rapid thermal processing
Appl. Phys. Lett. 99, 052103 (2011); 10.1063/1.3616145

Critical tensile and compressive strains for cracking of Al2O3 films grown by atomic layer deposition
J. Appl. Phys. 109, 084305 (2011); 10.1063/1.3567912

Density dependence of the room temperature thermal conductivity of atomic layer deposition-grown amorphous alumina (Al$_2$O$_3$)

Caroline S. Gorham,[1] John T. Gaskins,[1] Gregory N. Parsons,[2] Mark D. Losego,[2] and Patrick E. Hopkins[1,a)]

[1]*Department of Mechanical and Aerospace Engineering, University of Virginia, Charlottesville, Virginia 22904, USA*
[2]*Department of Chemical and Biomolecular Engineering, North Carolina State University, Raleigh, North Carolina 27695, USA*

We report on the thermal conductivity of atomic layer deposition-grown amorphous alumina thin films as a function of atomic density. Using time domain thermoreflectance, we measure the thermal conductivity of the thin alumina films at room temperature. The thermal conductivities vary $\sim$35% for a nearly 15% change in atomic density and are substrate independent. No density dependence of the longitudinal sound speeds is observed with picosecond acoustics. The density dependence of the thermal conductivity agrees well with a minimum limit to thermal conductivity model that is modified with a differential effective-medium approximation. © 2014 AIP Publishing LLC.
[http://dx.doi.org/10.1063/1.4885415]

For organic and biological devices, chemically stable, low thermal conductivity (κ) materials present a non-destructive means to provide thermal isolation.[1] A biologically stable,[1] chemically inert,[2–4] and low thermal conductivity[5] material commonly used in such devices is amorphous alumina (a-Al$_2$O$_3$). Similar to other amorphous materials,[6–10] the low thermal conductivity of a-Al$_2$O$_3$ is reduced further with sufficient reduction of atomic density (n). Deposition methods for growth of a-Al$_2$O$_3$, such as rf-sputtering,[11] dc-sputtering,[11] and atomic layer deposition (ALD), can create samples with a range of atomic densities depending on the growth conditions and kinetics. Therefore, in addition to providing insight into the role of atomic density on thermal conductivity, understanding the relationship between κ and n will provide validation of the quality of the various a-Al$_2$O$_3$ growth techniques.

In response, we measure the thermal conductivity of ALD-grown a-Al$_2$O$_3$ thin films as a function of atomic density. By varying the temperature during ALD, we synthesize a-Al$_2$O$_3$ thin films with atomic densities ranging from 2.66 to 3.07 $\pm$ 0.05 g/cm^3. We find that the thermal conductivity of ALD-grown a-Al$_2$O$_3$ varies appreciably with density; for a 13% change in volumetric mass density, the thermal conductivity varies nearly 35%. To elucidate the origin of the relationship between κ and n, we apply the differential effective-medium (DEM) approximation to the theoretical minimum limit to thermal conductivity.[12] At sufficiently high densities, the thermal conductivity is matched reasonably well by the minimum limit model. At lower densities, however, the data agree well with the DEM approximation, which attempts to describe altered material properties in heterogeneous solids of multiphase nature.[10] With picosecond acoustic measurements of sound speed in our ALD-grown a-Al$_2$O$_3$ thin films, we determine that reduction in sound velocity is not the origin of the density dependence of the thermal conductivity. Our data, when compared in context with previous measurements of the thermal conductivity of

rf and dc-sputter deposition-grown a-Al$_2$O$_3$ (Ref. 11), indicate that this strong density dependence of the thermal conductivity of ALD a-Al$_2$O$_3$ could be an intrinsic property of a-Al$_2$O$_3$.

The amorphous Al$_2$O$_3$ thin films were deposited onto single crystal (100) Si and z-cut quartz wafers by ALD in a custom-built, hot-walled, flow tube reactor. Nitrogen carrier gas flow (99.999% purity, National Welders) was metered with a mass flow controller to 300 SCCM and exhausted through a rotary vane pump. Precursor delivery was controlled electronically by a LabVIEW sequencer. Trimethylaluminum (TMA, Strem Chemicals) and reagent grade water (Ricca Chemicals) were used as precursors. Films were deposited at growth temperatures ranging from 50 °C to 250 °C to vary film density. All films were processed at 2 Torr of N$_2$ carrier gas using a sequence of 0.05 s TMA, 60 s N$_2$ purge, 0.05 s H$_2$O, 60 s N$_2$ purge for a total of 500 cycles. Film thickness and refractive index were assessed with a J. A. Woollam Alpha-SE Spectroscopic Ellipsometer using a Cauchy model. The refractive index of our thin films at 632.8 nm as a function of sample growth temperature is plotted in Fig. 1. The refractive index and atomic density of the Al$_2$O$_3$ thin films increase with growth temperature up to $\sim$150 °C, at which point a maximum refractive index of $\sim$1.66 is reached. These trends are consistent with prior reports.[1,13–18] Based on previous work relating the refractive index of a-Al$_2$O$_3$ to density,[19] we used the following calibration to relate our measured refractive index to the atomic density: $n = 5N_A(7.174\hat{n} - 8.76)/M$, which is valid for $1.50 < \hat{n} < 1.77$ at 632.8 nm. In this expression, $\hat{n}$ is the refractive index at 632.8 nm, N_A is Avogadro's number, and M is the molecular weight. The term in parenthesis represents the mass density of the a-Al$_2$O$_3$. The measured thicknesses, refractive indices, and calculated densities of our samples are presented in the Supplementary Material.[20]

We measured the thermal conductivities of the various samples with time-domain thermoreflectance (TDTR). The technique is described thoroughly in Refs. 21 and 22; thus,
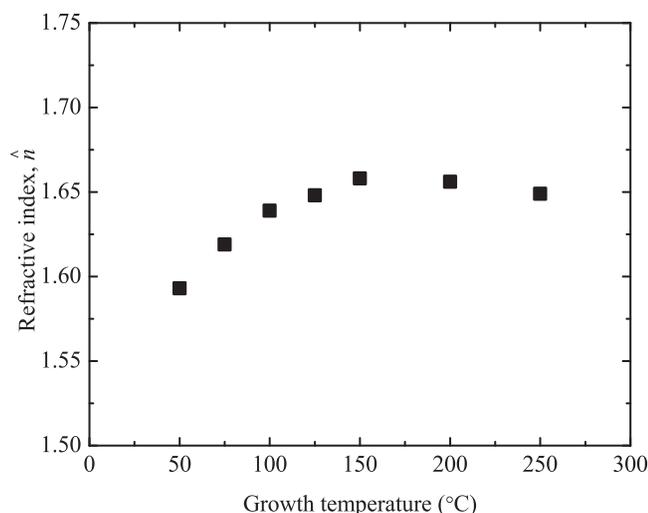
a)Electronic mail: phopkins@virginia.edu

FIG. 1. Refractive index, $\hat{n}$, at 632.8 nm versus growth temperature of ALD-grown a-Al$_2$O$_3$.
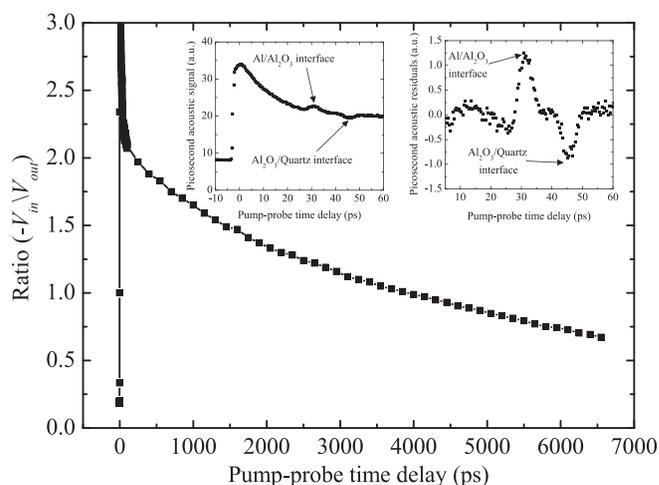

FIG. 2. TDTR data on the Al/a-Al$_2$O$_3$/quartz sample. The main figure shows the data that are used to determine the thermal conductivity of the a-Al$_2$O$_3$ film. The left and right insets, respectively, show the isolated picosecond acoustic response of the TDTR signal and the picosecond acoustic residuals. The positive and negative deviations from the exponential decay, as seen in the left inset, are indicative of a strain wave reflecting off of the Al/a-Al$_2$O$_3$ and a-Al$_2$O$_3$/quartz interfaces, respectively. The picosecond acoustic residuals, shown in the right inset, are determined by removing the exponential decay background from the TDTR signal. The positive "hump" and negative "dip," corresponding to the strain wave reflection off of the Al/a-Al$_2$O$_3$ and a-Al$_2$O$_3$/quartz interfaces, respectively, are clearly discernible from the residuals in the right inset.

we only briefly describe the technique here. TDTR is a non-contact optical pump-probe technique that uses a short-pulsed laser to both produce and monitor heating events on a surface of a sample. The laser output from our femtosecond oscillator is separated into "pump" and "probe" paths, in which the relative optical path lengths are adjusted with a mechanical delay stage. This system allows for picosecond temporal resolution of the thermoreflectivity on the sample surface. We frequency double the wavelength of the pump path to 400 nm to assist with optical filtering of the pump light.[22] The pump path is modulated at 11.39 MHz and a radio-frequency lock-in amplifier is used to detect the change in reflectivity of the probe beam at the modulation frequency of the pump heating event. The sample surface is coated with a thin aluminum film so that the change in reflectivity of the sample surface is an indication of the change in temperature of the Al transducer, which is driven by the thermal properties of the a-Al$_2$O$_3$ and the substrate. We monitor the ratio of the in-phase to out-of-phase voltage ($-V_{in}/V_{out}$). An example of a TDTR response on an Al/a-Al$_2$O$_3$/quartz sample is shown in Fig. 2.

Analyses accounting for pulse accumulation when using a Ti:sapphire oscillator, and the relationship between this temporal thermal response and the thermophysical properties of the sample, have been previously detailed.[21,23–25] In our measurements, the thermal response at the surface is related to the thermal conductivities and heat capacities of the Al transducer, the a-Al$_2$O$_3$ thin film and the substrate, along with the thermal boundary conductances across the Al/a-Al$_2$O$_3$ and a-Al$_2$O$_3$/substrate interfaces. We assume literature values for the heat capacities of each of the layers;[26,27] the heat capacities of the a-Al$_2$O$_3$ thin films are then scaled proportional to their reduced atomic densities. We use literature values for the thermal conductivities of the substrates.[28] Due to our pump and probe spot sizes (pump and probe $1/e^2$ radii of 25 μm and 10.5 μm, respectively) and our pump modulation frequency, we are not sensitive to κ of the Al transducer. We therefore have three unknowns in the model: the thermal boundary conductances across each interface and κ of a-Al$_2$O$_3$. However, we are negligibly sensitive to the

thermal boundary conductances at each interface due to a combination of the layer thicknesses, the low thermal conductivity of the a-Al$_2$O$_3$, and the modulation frequency of the pump beam. Thus, our measurements are most sensitive to κ of the a-Al$_2$O$_3$ thin films.

We use picosecond acoustic techniques to measure the longitudinal sound speeds in the a-Al$_2$O$_3$ thin films.[29,30] The sound speeds provide a relative measure of how the moduli of the a-Al$_2$O$_3$ thin films change with density. Piezoreflectance provides a signal in the TDTR response during the first few tens of picoseconds when the reflection of a laser-induced strain wave off of the Al/a-Al$_2$O$_3$ and a-Al$_2$O$_3$/substrate interfaces returns to the surface of the Al transducer. The reflection of the strain wave allows for measurement of the longitudinal sound speed of continuum vibrations in the a-Al$_2$O$_3$. Interpretation of the picosecond acoustic data is based on the acoustic impedances of the materials comprising the interface. As detailed previously,[31,32] if a strain wave in the metal film is reflected off of an interface of a material with a higher acoustic impedance than the metal film, the strain wave will experience a null phase shift and the reflected wave will increase the TDTR signal, i.e., it produces a "hump." However, if the material has a lower acoustic impedance than that of the metal film, the wave will undergo a π phase shift and will appear as a "dip" in the TDTR data.

As expected based on acoustic impedances for the Al/a-Al$_2$O$_3$ and a-Al$_2$O$_3$/quartz interfaces, we observe a "hump" followed by a "dip" in the picosecond acoustic response. An example of an isolated picosecond acoustic response and the picosecond acoustic residuals are plotted in the left-most and right-most inset of Fig. 2, respectively. From the time difference between the "hump" and "dip,"

along with the measured film thicknesses, we calculate the longitudinal sound speed of the a-Al$_2$O$_3$ samples to be $8700 \pm 160 \, \text{m s}^{-1}$, with no discernible differences or trends among the samples. The longitudinal speed of sound of a-Al$_2$O$_3$ has not previously been reported, however, our measured values are within 3% of the longitudinal speed of sound in α–phase alumina ceramic ($8800 \, \text{m s}^{-1}$).[33] The measured longitudinal sound speeds are given in the Supplementary Material;[20] it is noted that, due to the lack of a discernible trend in the measured sound speeds of the samples, the average value of $8700 \, \text{m s}^{-1}$ is considered for all samples. Since no density dependence of the longitudinal speed of sound is detected within the resolution of our experimental technique, due to the long-range isotropic nature of the amorphous systems, any density dependence of the shear modulus could be considered anomalous. Therefore, we adopt the transverse speed of sound of α–phase alumina ceramic for all of the samples considered.

Figure 3(a) plots the measured thermal conductivity as a function of atomic density for our ALD a-Al$_2$O$_3$ samples. Before discussing the results, we note that the thermal conductivities of the ALD a-Al$_2$O$_3$ thin films, presented in the Supplementary Material,[20] are independent of the substrate. We observe an appreciable dependence of the thermal conductivity on density: a ~15% change in density results in a ~35% change in thermal conductivity. A more pronounced density dependence was observed in previous measurements of thermal conductivity of a-Al$_2$O$_3$ thin films grown by Lee *et al.* (also shown in Fig. 3(a));[11] however, in the study by Lee *et al.* the variation with density was observed among samples grown by different techniques. Our results elucidate that this density dependence is intrinsic to ALD a-Al$_2$O$_3$. Furthermore, the samples measured by Lee *et al.* were much
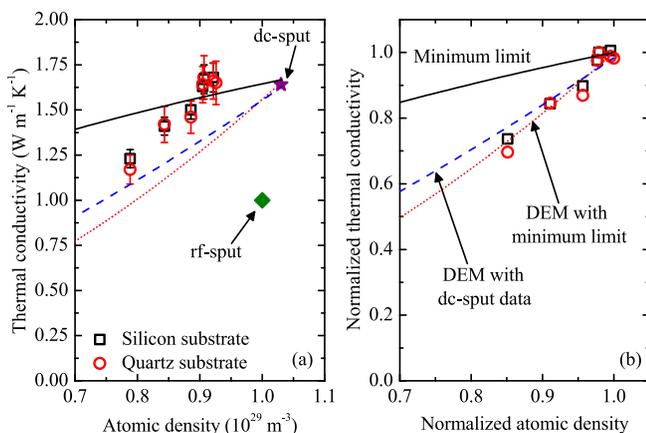

FIG. 3. (a) Measured room temperature thermal conductivity of our ALD-grown a-Al$_2$O$_3$ films on quartz (red circles) and Si (black squares) substrates as a function of atomic density of the sample. Thermal conductivity values reported by Lee *et al.*[11] for dc-sputter deposition-grown a-Al$_2$O$_3$ on crystalline Si (star) and rf-sputter deposition-grown a-Al$_2$O$_3$ on crystalline Si (diamond) are also plotted. Calculations of the minimum limit to thermal conductivity model, Eq. (1) (solid line),[12] the DEM approximation, Eq. (2), to the minimum limit model (dotted line) and the DEM approximation assuming the corresponding "fully dense" sample is the dc-sputtered sample reported by Lee *et al.*[11](dashed line) are also shown. (b) Normalized thermal conductivity of a-Al$_2$O$_3$ as a function of normalized density for the data reported in this work and the various models shown in (a). The density dependence in our measured values is captured well by the DEM approximations to thermal conductivity.

thicker than the samples studied here and given the relatively close agreement between our measurements and the thermal conductivity of the thicker dc-sputter deposition-grown a-Al$_2$O$_3$[11] we conclude that size effects do not affect κ in our ALD-grown a-Al$_2$O$_3$ samples at these thicknesses.[34]

As is clear from our measurements, alike other amorphous materials,[6–10] the thermal conductivity of a-Al$_2$O$_3$ decreases upon reduction of atomic density. To investigate the effect of atomic density on κ, we turn to the minimum limit to thermal conductivity[12] which has been used as a baseline model to compare to experimental data of amorphous systems for several decades. Within the framework of the minimum limit model, the lifetime of all oscillators is assumed to be one half of the period of vibration, i.e., $\tau = \pi/\omega$,[12] where ω is the angular frequency of oscillation. The thermal conductivity in this amorphous-limit approximation, κ_{min}, is the sum of three integrals accounting for three sound polarizations (one longitudinal and two transverse) given by

$$\kappa_{\text{min}} = \left(\frac{\pi}{6}\right)^{1/3} k_B n^{2/3} \sum_i c_i \left(\frac{T}{\Theta_i}\right)^2 \int_0^{\frac{\Theta_i}{T}} \frac{x^3 e^x}{(e^x - 1)^2} dx, \quad (1)$$

where i is the polarization index, c_i is the sound speed, Θ_i is the Debye temperature, defined as $\Theta_i = c_i(\hbar/k_B)(6\pi^2 n)^{1/3}$, k_B is the Boltzmann constant, $\hbar$ is the reduced Planck constant, and $x = \Theta_i/T$. As evident from Eq. (1), κ_{min} depends on only two material dependent parameters: the polarization-dependent continuum sound speeds and the atomic density of the material. We show calculations of Eq. (1) for a-Al$_2$O$_3$, at room temperature, as a function of atomic density as the solid line in Fig. 3(a). For these calculations, we use c_L from our picosecond acoustic measurements and c_T from Ref. 33. We note that our picosecond acoustic analysis confirms that the sound speed in a-Al$_2$O$_3$ is independent of atomic density for our samples. To further evaluate this form of the minimum limit to thermal conductivity applied to a-Al$_2$O$_3$, we normalize the calculations of Eq. (1) to our data, shown in Fig. 3(b). The density dependent thermal conductivity predictions of Eq. (1) do not capture the trends in our measured data.

In efforts to more closely describe the data over a larger density range, we apply the DEM approximation to the minimum limit model. DEM is an effective-medium approximation derived to account for the effects of multiphase nature on heterogeneous physical systems.[10,35] The DEM proposes that the thermal conductivity scales with atomic density as

$$\kappa_{\text{DEM}} = \left(\frac{n}{n_{\text{bulk}}}\right)^{3/2} \kappa. \quad (2)$$

Figure 3 plots Eq. (2) evaluating κ_{DEM} as a function of atomic density and assuming κ as either the measured value for the dc-sputtered film by Lee *et al.*[11] (dotted line) or κ_{min} explicitly from Eq. (1) (dashed line). For the calculations of Eq. (2) shown in Fig. 3(a), we assume a bulk atomic density of 1.0366×10^{29} atoms m^{-3}, corresponding to the highest density of a-Al$_2$O$_3$ measured by Lee *et al.*[11]

Clearly, the density dependence of the thermal conductivity trend in our ALD a-Al$_2$O$_3$ samples is steeper than that

predicted by Eq. (1), as is apparent by comparing the normalized data and models in Fig. 3(b). Both of our DEM-based thermal conductivity calculations exhibit much better agreement with our measured data than the traditional minimum limit approach (Eq. (1)). Furthermore, where the DEM calculations of thermal conductivity require the knowledge of the thermal conductivity of the "fully dense" phase of a-Al$_2$O$_3$, our approach of using the DEM with Eq. (1) only requires knowledge of atomic density and sound velocities. We have found similar agreement using this DEM-modified minimum limit approach to model low density silica,[9] demonstrating the promise in this modeling approach to predict the thermal conductivity of low density amorphous solids.

In summary, we have measured the room temperature thermal conductivity of ALD-grown a-Al$_2$O$_3$ thin films using time-domain thermoreflectance. The thermal conductivities of the thin alumina films at room temperature, which are substrate independent, vary by ~35% for a ~15% change in atomic density. We do not observe any density dependence of the longitudinal sound speeds as measured with picosecond acoustics. From this, we conclude that scaling of the sound speed is not the origin of the density dependence of κ over this density regime in amorphous alumina. The density dependence of the thermal conductivity agrees well with a minimum limit to thermal conductivity model that is modified with a differential effective-medium approximation.

[1]M. D. Groner, F. H. Fabreguette, J. W. Elam, and S. M. George, Chem. Mater. **16**, 639–645 (2004).

[2]G. T. Furukawa, T. B. Douglas, R. E. McCoskey, and D. C. Ginnings, J. Res. Nat. Bur. Stand. **57**, 67–82 (1956).

[3]R. Heid, D. Strauch, and K.-P. Bohnen, Phys. Rev. B **61**, 8625–8627 (2000).

[4]D.-A. Borca-Tasciuc and G. Chen, J. Appl. Phys. **97**, 084303 (2005).

[5]P. Vashishta, R. K. Kalia, A. Nakano, and J. P. Rino, J. Appl. Phys. **103**, 083504 (2008).

[6]J. Fricke, X. Lu, P. Wang, D. Buttner, and U. Heinemann, Int. J. Heat Mass Transfer **35**, 2305–2309 (1992).

[7]C. Hu, M. Morgen, P. S. Ho, A. Jain, W. N. Gill, J. L. Plawsky, J. Peter, and C. Wayner, Appl. Phys. Lett. **77**, 145–147 (2000).

[8]A. J. Bullen, K. E. O'Hara, D. G. Cahill, O. Monteiro, and A. von Keudell, J. Appl. Phys. **88**, 6317–6320 (2000).

[9]P. E. Hopkins, B. Kaehr, E. S. Piekos, D. Dunphy, and C. J. Brinker, J. Appl. Phys. **111**, 113532 (2012).

[10]R. M. Costescu, A. J. Bullen, G. Matamis, K. E. O'Hara, and D. G. Cahill, Phys. Rev. B **65**, 094205 (2002).

[11]S.-M. Lee, D. G. Cahill, and T. H. Allen, Phys. Rev. B **52**, 253 (1995).

[12]D. G. Cahill, S. K. Watson, and R. O. Pohl, Phys. Rev. B **46**, 6131–6140 (1992).

[13]J.-F. Fan, K. Sugioka, and K. Toyoda, Jpn. J. Appl. Phys. **30**, L1139 (1991).

[14]H. Kattelus, M. Ylilammi, J. Saarilahti, J. Antson, and S. Lindfors, Thin Solid Films **225**, 296 (1993).

[15]K. Kukli, M. Ritala, M. Leskelä, and J. Jokinen, J. Vac. Sci. Technol. A **15**, 2214 (1997).

[16]S. J. Yun, K.-H. Lee, J. Skarp, H.-R. Kim, and K.-S. Nam, J. Vac. Sci. Technol. A **15**, 2993 (1997).

[17]A. W. Ott, J. W. Klaus, J. M. Johnson, and S. M. George, Thin Solid Films **292**, 135 (1997).

[18]R. Matero, A. Rahtu, M. Ritala, M. Leskelä, and T. Sajavaara, Thin Solid Films **368**, 1 (2000).

[19]K. K. Shih and D. B. Dove, J. Vac. Sci. Technol. A **12**, 321 (1994).

[20]See supplementary material at http://dx.doi.org/10.1063/1.4885415 for a table of relevant physical properties for the samples studied.

[21]D. G. Cahill, Rev. Sci. Instrum. **75**, 5119–5122 (2004).

[22]P. E. Hopkins, M. Ding, and J. Poon, J. Appl. Phys. **111**, 103533 (2012).

[23]A. J. Schmidt, X. Chen, and G. Chen, Rev. Sci. Instrum. **79**, 114902 (2008).

[24]P. E. Hopkins, J. R. Serrano, L. M. Phinney, S. P. Kearney, T. W. Grasser, and C. T. Harris, J. Heat Transfer **132**, 081302 (2010).

[25]P. E. Hopkins, B. Kaehr, L. M. Phinney, D. Dunphy, C. J. Brinker, F. Garcia, T. P. Koehler, and A. M. Grillet, J. Heat Transfer **133**, 061601 (2011).

[26]Y. S. Touloukian and E. H. Buyco, *Thermophysical Properties of Matter-Specific Heat: Metallic Elements and Alloys* (IFI/Plenum, New York, 1970), Vol. 4.

[27]Y. S. Touloukian and E. H. Buyco, *Thermophysical Properties of Matter-Specific Heat: Nonmetallic Solids* (IFI/Plenum, New York, 1970), Vol. 5.

[28]Y. S. Touloukian, R. W. Powell, C. Y. Ho, and P. G. Klemens, *Thermophysical Properties of Matter-Thermal Conductivity: Nonmetallic Solids* (IFI/Plenum, New York, 1970).

[29]C. Thomsen, J. Strait, Z. Vardeny, H. J. Maris, J. Tauc, and J. J. Hauser, Phys. Rev. Lett. **53**, 989–992 (1984).

[30]C. Thomsen, H. T. Grahn, H. J. Maris, and J. Tuac, Phys. Rev. B **34**, 4129 (1986).

[31]C. Chiritescu, "Ultra low thermal conductivity in layered disordered crystalline materials," Ph.D. thesis, University of Illinois at Urbana-Champaign, 2010.

[32]G. T. Hohensee, W.-P. Hsieh, M. D. Losego, and D. G. Cahill, Rev. Sci. Instrum. **83**, 114902, (2012).

[33]C. T. Lynch, *Practical Handbook of Materials Science* (CRC press, 1989).

[34]R. Cheaito, J. C. Duda, T. E. Beechem, K. Hattar, J. F. Ihlefeld, D. L. Medlin, M. A. Rodriguez, M. J. Campion, E. S. Piekos, and P. E. Hopkins, Phys. Rev. Lett. **109**, 195901 (2012).

[35]D. A. G. Bruggeman, Ann. Phys. **416**(7), 636–664 (1935).